Inclusion crystals of 2,2′,7,7′,9,9′-hexahalo-9,9′-bisfluorenyl derivatives: a new family of polyhalo aryl hosts

Koichi Tanaka,[a,*] Shin-ichi Wada[a] and Mino R. Caira[b,*]

[a]Department of Chemistry and Materials Engineering, Faculty of Chemistry, Materials and Bioengineering & High Technology
Research Center, Kansai University, Suita, Osaka 564-8680, Japan
[b]Department of Chemistry, University of Cape Town, Rondebosch 7701, South Africa

Abstract—The preparation and inclusion properties of the new halo aryl hosts, 2,2′,7,7′,9,9′-hexahalo-9,9′-bisfluorenyl derivatives **5–7**, are described. The host compounds **5–7** having four halogen atoms on the aromatic rings form stable inclusion crystals with many guest compounds, whereas the parent compound **4** does not. The X-ray structures of the host **4** and representative inclusion compounds of hosts **5–7** were determined, allowing rationalization of several of the experimental observations.
© 2007 Elsevier Ltd. All rights reserved.

1. Introduction

There has been increasing interest in host–guest inclusion compounds because of their potential applications such as separation of isomeric compounds, optical resolution of enantiomers, reaction medium of included molecules, and sensor materials.[1] The classical hydrogen bond, one of the strong intermolecular interactions, has been widely utilized in the arrangement of host and guest molecules in crystalline lattices. More recently, however, a new family of lattice inclusion hosts, polyhalo aryl host compounds, utilizing

weaker halogen–halogen interactions has been discovered. We reported tetrahalophenyl ethylene derivatives **1b–1e**,[2–5] and Bishop[6–8] reported V-shaped diquinoline derivatives **2b–2c** and **3b** as efficient host molecules. The compounds **1b–1e**, **2b–2c**, and **3b** show inclusion properties, but their corresponding hydrocarbons **1a**, **2a**, and **3a** do not include any guest molecules. We report here the preparation and inclusion properties of new polyhalo aryl host compounds, 2,2′,7,7′,9,9′-hexahalo-9,9′-bisfluorenyl derivatives **5–7**.
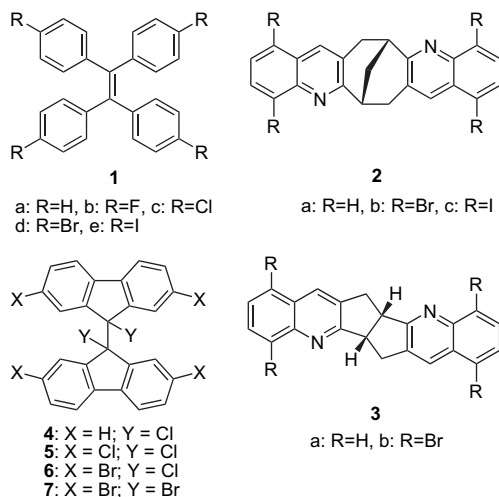
2. Results and discussion

2.1. Preparation of the host compounds 4–7

2,2′,7,7′,9,9′-Hexachloro-9,9′-bisfluorenyl **5** was prepared by the coupling reaction of 2,7,9,9-tetrachloro-9*H*-fluorene using copper powder. 2,2′,7,7′-Tetrabromo-9,9′-dichloro-9,9′-bis-fluorenyl **6**[9] and 2,2′,7,7′,9,9′-hexabromo-9,9′-bisfluorenyl **7**[9] were prepared by bromination of 9,9′-dichloro-9,9′-bis-fluorenyl **4**[9] and 9,9′-bisfluorenylidene, respectively.

2.2. Inclusion properties

A wide variety of organic solvents including halogenated alkanes, halogenated aromatic compounds, aromatic hydro-carbons, and cyclic ethers were used for the inclusion experiments (Table 1). The most efficient host was 2,2′,7,7′-tetrabromo-9,9′-dichloro-9,9′-bisfluorenyl **6** fol-lowed by 2,2′,7,7′,9,9′-hexabromo-9,9′-bisfluorenyl **7**, while 2,2′,7,7′,9,9′-hexachloro-9,9′-bisfluorenyl **5** was less effec-tive and included only aromatic compounds. Host **6** includes

1
a: R=H, b: R=F, c: R=Cl
d: R=Br, e: R=I

2
a: R=H, b: R=Br, c: R=I

4: X = H; Y = Cl
5: X = Cl; Y = Cl
6: X = Br; Y = Cl
7: X = Br; Y = Br

3
a: R=H, b: R=Br

* Corresponding authors. Tel./fax: +81 6 6368 0861; e-mail: ktanaka@ipcku.kansai-u.ac.jp

Table 1. Host–guest ratios and guest release temperatures of the inclusion crystals of **4–7**

Guest	4	5	6	7
CH_3I	—[a]	—	2:3, 77–92	1:2, 81–102
CH_2Cl_2	—	—	1:1, 98–108	1:1, 55–131
CH_2Br_2	—	—	1:1, 97–113	1:1, 75–145
$CHCl_3$	—	—	1:1, 98–106	1:1, 49–131
CCl_4	—	—	—	1:1, 113–123
C_2H_5Br	—	—	1:1, 93–104	1:1, 51–141
C_2H_5I	—	—	1:1, 93–103	—
1,2-Dichloroethane	—	—	1:1, 97–112	1:1, 54–81
1,2-Dibromoethane	—	—	2:1, 99–129	1:1, 85–107
1,2-Dibromocyclohexane	—	—	—	1:1, 109–128
Chlorobenzene	—	2:1,[b] 109–124[c]	2:1, 115–157	—
Bromobenzene	—	—	2:1, 110–178	—
Iodobenzene	—	2:1, 126–154	2:1, 130–176	1:1, 92–104
Benzyl chloride	—	—	1:1, 71–126	1:1, 86–93
Benzyl bromide	—	—	1:1, 85–193	1:1, 97–111
o-Bromotoluene	—	—	2:1, 102–117	—
m-Bromotoluene	—	—	2:1, 110-140	—
p-Bromotoluene	—	2:1, 97–177	2:1, 102–205	2:1, 158–180
p-Bromoanisole	—	2:1, 132–223	2:1, 185–209	2:1, 125–192
Benzene	—	—	2:3, 79–87	2:3, 97–108
Toluene	—	2:1, 111–124	2:1, 124–147	—
o-Xylene	—	—	2:1, 122–136	—
m-Xylene	—	—	2:1, 102–112	—
p-Xylene	—	2:1, 89–172	2:1, 160–187	2:1, 131–143
Tetrahydrofuran	—	—	1:1, 79–97	1:1, 81–111
Tetrahydropyrane	—	—	—	1:1, 96–117
Dioxane	—	—	2:3, 49–114	2:3, 84–91

[a] No inclusion.
[b] Host–guest ratios were determined by TG and ^{1}H NMR.
[c] Guest release temperature (°C).

a wide range of halogenated alkanes, halogenated aromatic compounds, aromatic compounds, and some cyclic ethers. In contrast, 9,9′-dichloro-9,9′-bisfluorenyl **4** did not form any inclusion crystals with the guest molecules listed in Table 1. This suggests that the halogen atoms, especially bromine atoms on aromatic rings, play an important role for efficient inclusion of guest molecules. It is also remarkable that host **6** forms stable inclusion crystals with halogenated guest compounds and the guest molecules are liberated at much higher temperatures than their guest boiling points (Table 1). For example, a 1:1 inclusion crystal of **6** with chloroform decomposed when the inclusion crystal was heated above 98 °C, although the boiling point of chloroform is only 61 °C (Fig. 1, TG).

Another interesting difference between the inclusion behavior of hosts **5** and **7** is the selectivity toward the isomeric compounds. For example, hosts **5** and **7** include only the *p*-isomers of xylene and bromotoluene in 2:1 ratios, while

host **6** shows no preference and includes *o*-, *m*-, and *p*-isomers of these compounds in 2:1 ratios in each case.

2.3. X-ray structural analyses

Following isolation of high-quality single crystals of the host compound **4**, as well as the inclusion complexes **5**·(*p*-xylene)$_{0.5}$, **6**·CHCl$_3$, **7**·CHCl$_3$, and **7**·1,2-dibromocyclohexane, their single crystal X-ray structures were determined in order to shed light on some of the experimental observations above. Crystal data and refinement parameters for these species appear in Tables 2 and 3.

Given the structural similarities in host compounds **5–7**, some degree of isostructurality of their inclusion complexes
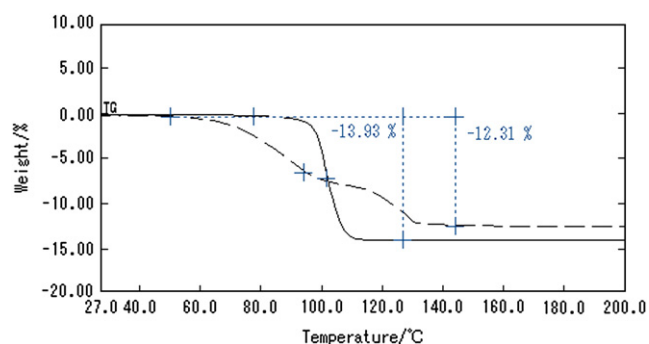

Figure 1. TG traces of **6**·CHCl$_3$ (solid line) and **7**·CHCl$_3$ (broken line).

Table 2. Crystal data and refinement parameters for host **4** and the inclusion complex **5**·(*p*-xylene)$_{0.5}$

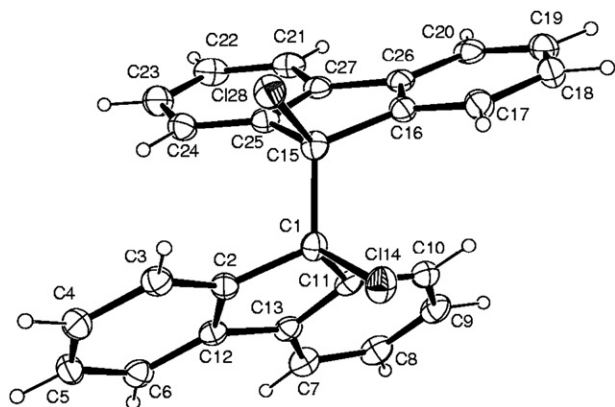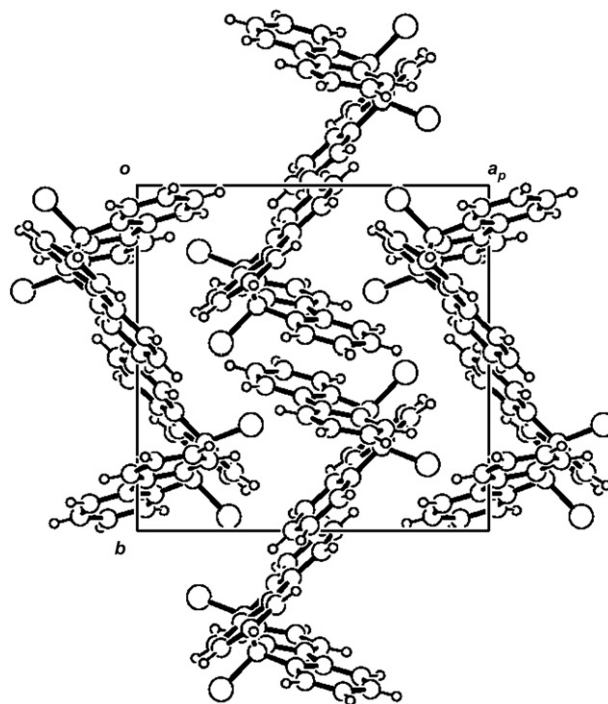|	4	5·(*p*-xylene)$_{0.5}$
Formula	$C_{26}H_{16}Cl_2$	$C_{26}H_{12}Cl_6 \cdot (C_8H_{10})_{0.5}$
Formula weight	399.29	590.14
Crystal system	Monoclinic	Triclinic
Space group	$P2_1/n$	$P(-1)$
a, Å	9.3289(2)	9.7489(2)
b, Å	11.9856(1)	12.1816(2)
c, Å	12.6858(2)	12.6908(2)
α, °	90.0	61.972(1)
β, °	103.029(1)	87.023(1)
γ, °	90.0	76.336(1)
Z	4	2
T, K	113(2)	113(2)
λ, Å	0.71073 (Mo Kα)	0.71073 (Mo Kα)
R_1	0.0328	0.0346
wR_2	0.0860	0.0741
Goodness of fit	1.050	0.974

Table 3. Crystal data and refinement parameters for the inclusion complexes **6**·CHCl₃, **7**·CHCl₃ and **7**·1,2-dibromocyclohexane

	6·CHCl₃	**7**·CHCl₃	**7**·1,2-dibromo-cyclohexane
Formula	$C_{26}H_{12}Cl_2Br_4$·CHCl₃	$C_{26}H_{12}Br_6$·CHCl₃	$C_{26}H_{12}Br_6$·$C_6H_{10}Br_2$
Formula weight	834.26	923.18	1045.78
Crystal system	Triclinic	Triclinic	Monoclinic
Space group	$P(-1)$	$P(-1)$	$C2/c$
a, Å	9.7690(1)	10.7771(2)	13.0235(2)
b, Å	12.6480(1)	11.9491(2)	17.6229(2)
c, Å	12.9655(2)	11.9665(3)	15.1527(2)
α, °	62.670(1)	84.608(1)	90.0
β, °	86.520(1)	71.948(1)	110.557(1)
γ, °	74.257(1)	75.750(1)	90.0
Z	2	2	4
T, K	113(2)	113(2)	223(2)
λ, Å	0.71073 (Mo Kα)	0.71073 (Mo Kα)	0.71073 (Mo Kα)
R_1	0.0447	0.0356	0.0407
wR_2	0.0804	0.0813	0.0920
Goodness of fit	1.032	1.033	1.038

was expected. Close similarity in the unit cell parameters for **5**·(*p*-xylene)₀.₅ and **6**·CHCl₃ and their common space group suggested that the host molecules might adopt isostructural frameworks in the crystals, despite the different nature of the included guests. This feature was confirmed and is discussed in detail below.
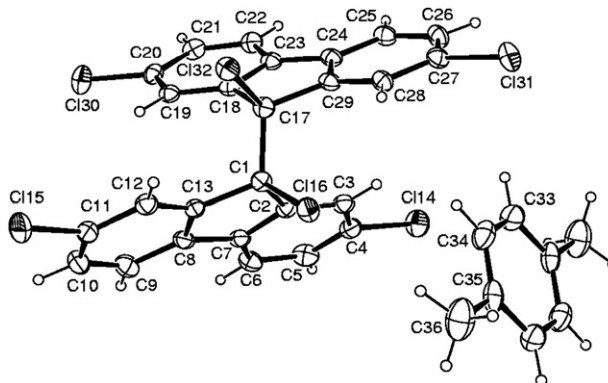
Figure 2 shows the asymmetric unit in the structure of the host compound **4**.

Each tricyclic moiety is slightly bowed in the direction of its bonded chlorine atom with the phenyl groups inclined at 3.5(1)° and 7.4(1)° for the moieties associated with Cl14 and Cl28, respectively. The two C–Cl distances are identical at 1.811(2) Å and the torsion angle describing the overall conformation, Cl14–C1–C15–Cl28, is −58.1(1)° for the molecule shown. This conformation is stabilized by two equivalent intramolecular hydrogen bonds, C17–H···Cl14 and C3–H···Cl28 with H···Cl distance ~2.8 Å. Only one intermolecular π-stacking interaction with centroid···centroid (Cg···Cg) distance less than 4 Å occurs in the crystal structure (Fig. 3), namely that between a five-membered ring of one molecule and a phenyl ring of a symmetry-related molecule (1−*x*, 1−*y*, 1−*z*) with Cg···Cg distance 3.916(1) Å.

Figure 3. Projection down the crystal *c*-axis of the packing of the molecules of host compound **4**.

For the inclusion complex **5**·(*p*-xylene)₀.₅ the asymmetric unit comprises one molecule of host **5** and one half of a molecule of *p*-xylene (Fig. 4), the guest molecule being located on the center of inversion.

Similar bowing of the tricyclic moieties to that observed in host molecule **4** occurs in **5**. The corresponding torsion angle defining the overall conformation of host **5** (Cl16–C1–C17–Cl32=−61.3(2)°) is also very similar to that in host **4**. In both cases, this conformation is determined by the short intramolecular Cl···Cl contact distances (3.289(1) Å in **4**, 3.307(1) Å in **5**) and intramolecular hydrogen bonds C–H···Cl with H···Cl distance ~2.8 Å. The Csp^3–Cl bond lengths in host **5** (1.808(2) and 1.812(2) Å) do not differ significantly from those in host **4**, while the aromatic C–Cl distances in **5** span the narrow range of 1.734(3)–1.744(3) Å. There is one crystallographically unique intermolecular π-stacking interaction with Cg···Cg distance less than 4 Å

Figure 2. The molecule of host compound **4** with atom labeling and thermal ellipsoids shown at the 50% probability level.

Figure 4. Host and guest molecules in **5**·(*p*-xylene)₀.₅. Atoms of the asymmetric unit are labeled and the thermal ellipsoids are drawn at the 50% probability level.

between host molecules, namely that between the phenyl rings C2→C7 at x, y, z and C8→C13 at $-x$, $2-y$, $1-z$, with Cg⋯Cg=3.705 Å. Two identical interactions of this type link the two inversion-related molecules.

In the crystal of the inclusion complex **5**·(p-xylene)$_{0.5}$, each guest molecules is located in a distinct cavity. Identical cavities have their centers at unit translations (i.e., intervals of ∼9.75 Å) along the line x, 1/2, 1/2 in Figure 5.

Details of the encapsulation of guest molecules by surrounding host molecules are shown in Figure 6, where host and guest molecules are drawn in ball-and-stick and space-filling modes, respectively. Apart from two (host)C–H⋯Cg(p-xylene) interactions with H⋯C ∼2.9 Å, there are no strong host–guest interactions and the compound **5**·(p-xylene)$_{0.5}$ may be described as a clathrate. Each guest methyl group makes contact with the open end of a V-shaped host molecule. Host chlorine atoms (both those attached to Csp^3 and Csp^2 atoms) are located in close vicinity of the guest molecule, contributing to its enclathration. In particular, it is the aromatic chlorine atom substituents in host **5** that act as barriers between contiguous cavities containing the guest molecules. This structural feature is consistent with the earlier experimental observation that incorporation of aromatic halogen atoms in the dihalo-9,9′-bisfluorenyl motif enhances clathration ability. In contrast to host molecule **5**, host **4** contains only Csp^3-bonded chlorine atoms and is evidently able to pack efficiently in the space group $P2_1/c$ without incorporating solvent molecules in the crystal.

The asymmetric unit in the inclusion compound **6**·CHCl$_3$ is shown in Figure 7, whose close resemblance to Figure 4 reflects the isostructurality between **6**·CHCl$_3$ and **5**·(p-xylene)$_{0.5}$ referred earlier.

Replacement of the four aromatic chlorine atoms in host **5** by bromine atoms in host **6** results in retention of both the
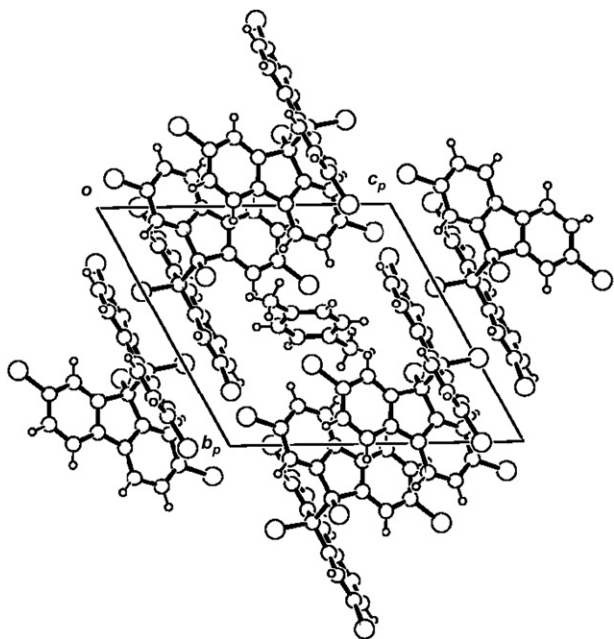

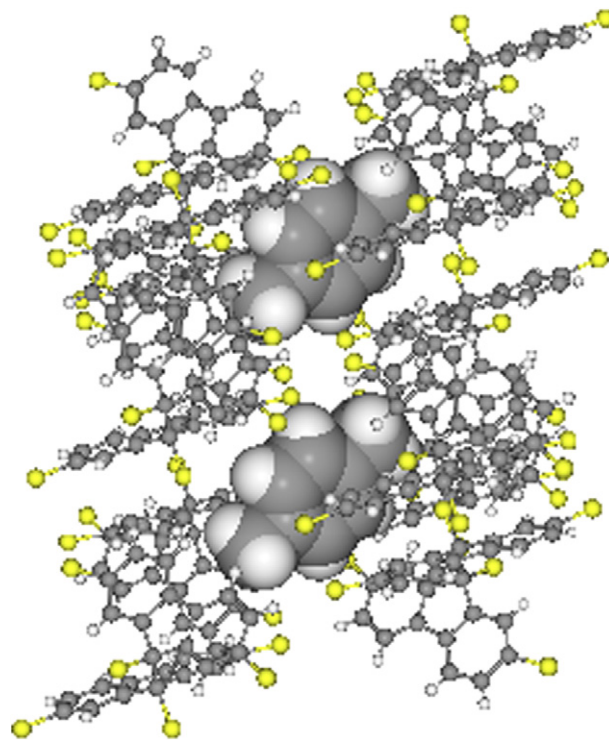**Figure 6**. Encapsulation of p-xylene molecule by host molecules in the inclusion complex **5**·(p-xylene)$_{0.5}$.

molecular conformation as well as the mode of inclusion of the guest molecules in the crystal. In host molecule **6**, the C–Cl distances are 1.812(3) and 1.817(3) Å, i.e., not significantly different from the corresponding distances in the previous two compounds. The C–Br distances span the narrow range 1.892(4)–1.906(4) Å.

Encapsulation of the guest CHCl$_3$ molecules in the inclusion compound **6**·CHCl$_3$ is shown in Figure 8. Each cavity contains two CHCl$_3$ molecules, related by an inversion center. Comparison of Figures 6 and 8 reveals that isostructurality results from the similarity in steric bulk of this pair of molecules and that of a p-xylene molecule. The cavities in the crystal of **6**·CHCl$_3$ are separated from one another primarily by the Br atoms attached to the phenyl rings of host **6**. The inclusion of chloroform molecules in **6**·CHCl$_3$ is assisted

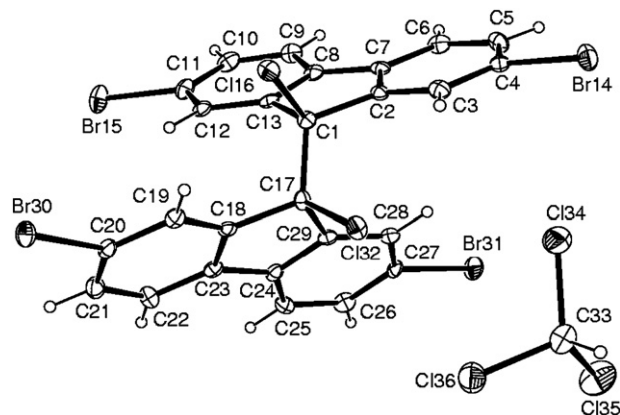**Figure 5**. Crystal packing of the inclusion complex **5**·(p-xylene)$_{0.5}$ viewed down [100].

Figure 7. The asymmetric unit in the inclusion compound **6**·CHCl$_3$ with thermal ellipsoids at the 50% probability level.
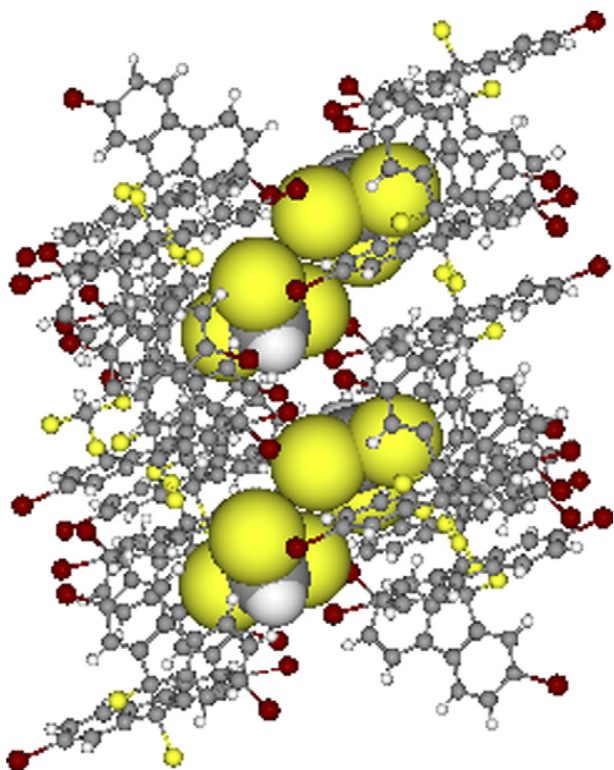
Figure 8. Encapsulation of CHCl$_3$ molecules by host molecules in the inclusion complex **6**·CHCl$_3$. (Color code: Cl yellow, Br brown).

Figure 9. The asymmetric unit in the inclusion compound **7**·CHCl$_3$ with thermal ellipsoids at the 50% probability level.

by the formation of a host–guest hydrogen bond C33–H···Br31^i ($i=1-x$, $-y$, $1-z$) with H···Br 2.86 Å and C···Br 3.649(4) Å.

The exceptional thermal stability of the inclusion compound **6**·CHCl$_3$, referred earlier and reflected in a guest-release temperature exceeding the boiling point of the pure solvent CHCl$_3$ by nearly 40°, can be attributed to several factors evident from the X-ray analysis. These include the location of chloroform molecules in isolated sites in the crystal, host–guest hydrogen bonding, and both host–host and host–guest halogen bonding that include the respective interactions C–Br···Br–C (with Br···Br 3.67 Å) and C–Br···Cl–C (in the range 3.56–3.77 Å). While the mode of encapsulation of *p*-xylene molecules in its complex with host **5** is virtually identical, host–guest hydrogen bonding and halogen bonding are not evident, and in this case guest-release actually commences at a lower temperature than the boiling point of *p*-xylene (138 °C) but is only complete at a significantly higher temperature (Table 1).

As in compound **6**·CHCl$_3$, the asymmetric unit in the crystal of the inclusion compound **7**·CHCl$_3$ again consists of one host molecule and one chloroform molecule (Fig. 9). The host molecule adopts the same conformation (approximately C_2) as those of the previously described hosts, with a torsion angle Br27–C1–C14–Br28=$-57.9(4)$°. Bond distances C–Br fall into two distinct groups. Csp^3–Br (1.973(5) and 1.982(5) Å) and Csp^2–Br (range 1.894(5)–1.906(5) Å).

Comparison of the unit cell data of **7**·CHCl$_3$ and **6**·CHCl$_3$ suggests that they may share similar packing features. A study of various projections indicated some similarities in
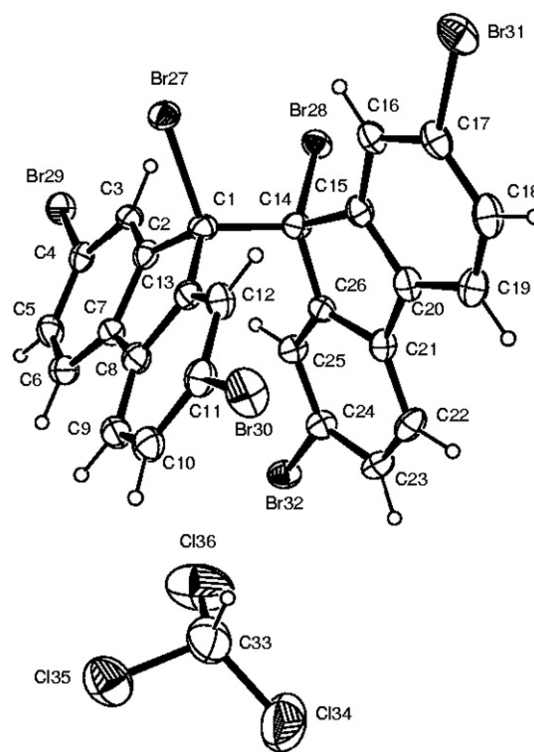
the packing arrangements but an analysis of guest–guest contact distances showed that the guest molecules in **7**·CHCl$_3$ are aligned in continuous channels (Fig. 10) rather than being confined within isolated cavities. Whereas in the crystal of **6**·CHCl$_3$ the closest alternate intermolecular guest Cl···Cl distances are ∼3.8 and 6.9 Å, consistent with cavity containment in pairs, the orientations of the chloroform molecules in the crystal of **7**·CHCl$_3$ are such that the corresponding Cl···Cl distances are ∼3.6 and 3.8 Å, i.e., the guest molecules are in contact, occupying a continuous channel parallel to the *b*-axis.

The replacement of the host Cl atoms in molecule **6** by Br atoms to yield the fully brominated host **7**, therefore has a significant effect on the encapsulation of chloroform molecules, changing the mode of guest inclusion from 'isolated site' to 'channel' type. The shortest host(Br)···guest(Cl) distances are in the range 3.6–3.8 Å.

In this case, the presence of guest molecules in channels, rather than in isolated sites, is consistent with the relatively low onset temperature of guest-release (Table 1).

The X-ray structure of the inclusion compound between host molecule **7** and 1,2-dibromocyclohexane was also determined. A 1:1 host–guest stoichiometry and $Z=4$ in the space group *C*2/*c* require both the host and guest molecules to occupy special positions, and both were located on a twofold rotation axis. Figure 11 shows the structure of the host molecule.

The Br–C–C–Br torsion angle is 58.3(4)° (or $-58.3(4)$° for comparison with the host molecule of opposite handedness

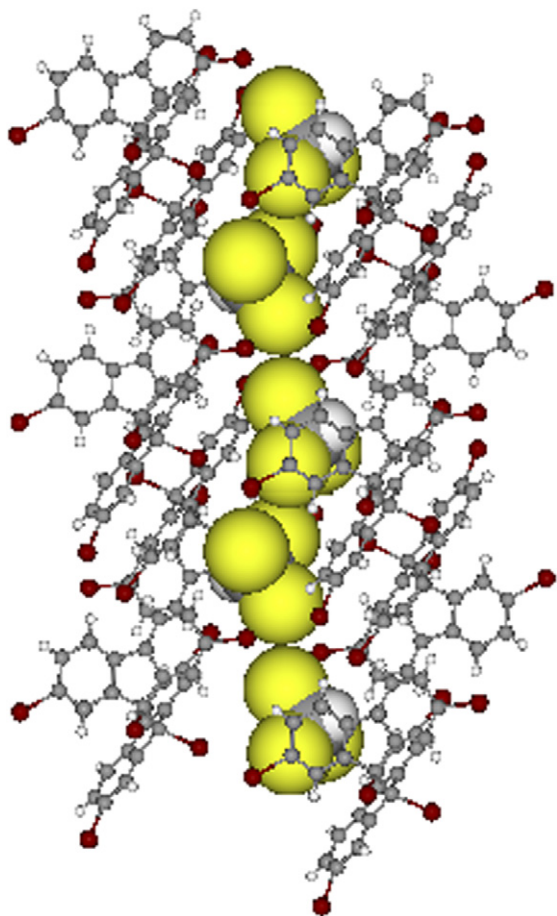**Figure 10**. Inclusion of chloroform molecules in a representative channel in the compound **7**·CHCl₃.

shown in Fig. 9) and the bond distances are C1–Br16 1.980(5), C4–Br14 1.903(6), and C11–Br15 1.898(6), in agreement with those found in the compound **7**·CHCl₃. Two symmetry-equivalent intramolecular hydrogen bonds C3–H···Br16 with H···Br 2.87 Å stabilize the host conformation. The relative sizes of the host thermal ellipsoids in

Figures 9 and 11 reflect the different temperatures at which the structures were determined (Table 3). Attempts to determine the structure of **7**·1,2-dibromocyclohexane from data collected at 113 K were unsuccessful due to a phase transition occurring in that temperature region. This transition was not, however, investigated in detail.

Resolution of the guest structure was complicated by its twofold disorder coupled with its location on a crystallographic twofold axis (Fig. 12) and several distance constraints and isotropic thermal modeling were necessary for satisfactory refinement. However, each member of the disordered pair revealed a chair conformation for the cyclohexane ring (with one carbon atom on the C_2 axis shared between the two rings) and a 1,2-diaxial orientation of the bromine substituents.

The Br atoms of the guest molecule are wedged within the wide end of the V-shaped host molecule and the inclusion complex packing viewed along [001] is shown in Figure 13. In this projection, the guest molecules appear to form cyclic arrays that enclose host molecules. Further examination of the structure revealed that the guest molecules are arranged in linear channels parallel to [101], along which C–Br···Br–C Type I interactions, involving the disordered bromine atoms, occur with Br···Br ∼3.60 Å. Host molecules are likewise linked to one another in infinite chains in this direction by C4–Br14···Br15′–C11′ Type II interactions with Br···Br ∼3.66 Å. The crystal structure is thus characterized by channel-packing of guest molecules and stabilizing host–host and guest–guest Br···Br interactions. Inclusion of guest molecules within continuous channels can be reconciled with the observed low onset temperature of guest-release upon heating (Table 1). This temperature is considerably lower than the boiling point of the pure solvent (∼145 °C at 100 mmHg).

3. Conclusion

For the novel hosts reported here, there is some degree of selectivity as regards the nature of the guest molecules that they include, and the guest-release data provided indicate
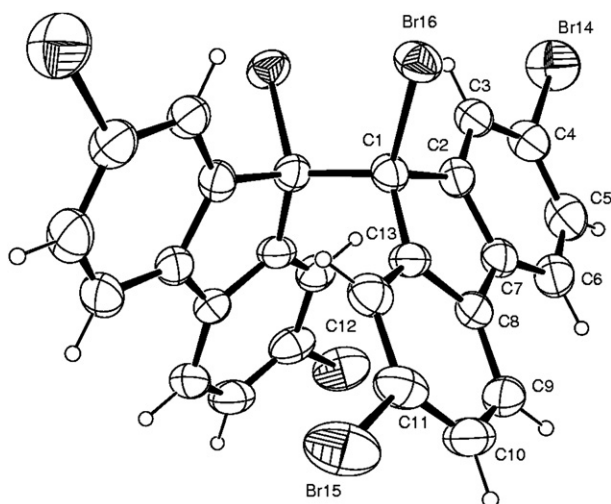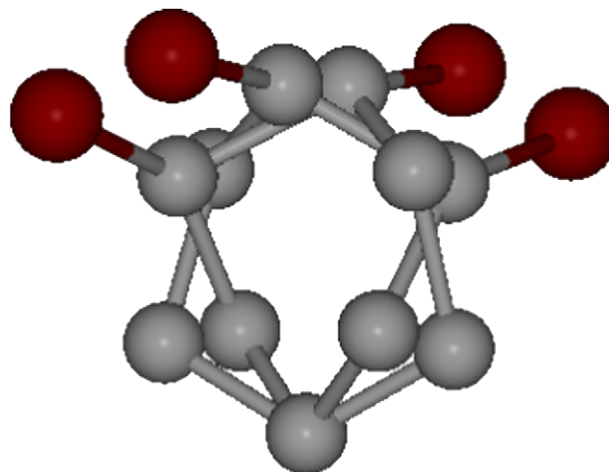

Figure 11. Conformation of the host molecule **7** in its inclusion complex with the guest 1,2-dibromocyclohexane. Thermal ellipsoids are drawn at the 50% probability level.

Figure 12. Disordered model of the guest 1,2-dibromocyclohexane in its inclusion compound with host **7**. The crystallographic C_2 axis is vertical and H atoms are omitted for clarity.
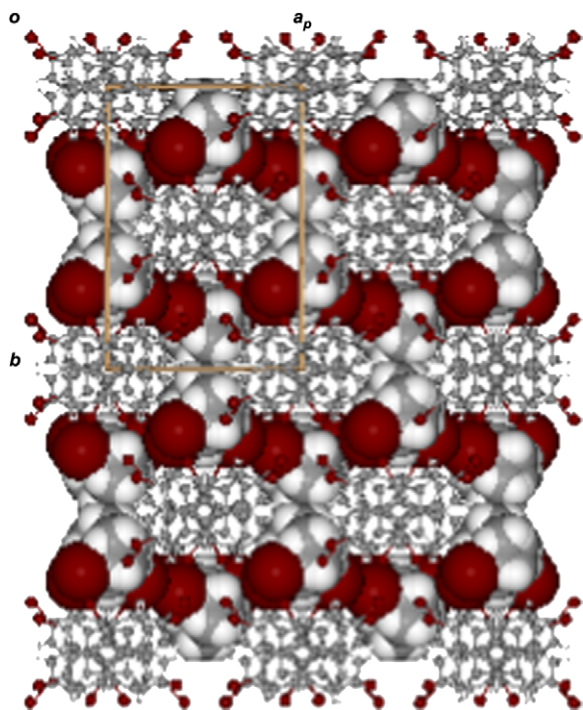
Figure 13. Crystal packing in the 1:1 inclusion compound between host **7** and 1,2-dibromocyclohexane. Host and guest molecules are drawn in ball-and-stick and space-filling modes, respectively. Four unit cells are shown.

that the resulting inclusion compounds display a wide range of thermal stabilities. X-ray analysis has shown that the host molecules **4**–**7** generally adopt a conformation with C_2 symmetry, which is stabilized by intramolecular C–H···Cl or C–H···Br hydrogen bonds. The torsion angle X–C–C–X (X=Cl, Br) defining the overall host conformation varies within a very narrow range (magnitudes 57.9–61.3°) for the five crystals examined. All compounds crystallized with both host enantiomeric forms present. The X-ray results support the notion that the more highly halogenated hosts **5**–**7** are generally more successful in including guest molecules due to their ability to form favorable halogen···halogen interactions (host–host and host–guest, when the latter is possible). For the inclusion compounds whose structures were determined, it was possible to rationalize the observed thermal behaviors qualitatively on the basis of the type of guest inclusion mode ('isolated site', 'channel' inclusion), as well as the observed hydrogen bonding and halogen bonding interactions. This approach was particularly useful in the attempt to find reasons for the significant difference in thermal behavior of the compounds **5**·(*p*-xylene)$_{0.5}$ and **6**·CHCl$_3$, which are based on nearly isostructural host frameworks.

4. Experimental

4.1. General

^{1}H NMR spectra were recorded in CDCl$_3$ on a JEOL JNM-EX270 FTNMR spectrometer. IR spectra were recorded with a JASCO FTIR 4100 spectrometer. Thermogravimetric (TG) analyses were performed on a Rigaku TG-8120 instrument. The inclusion crystals were obtained by recrystallization of the host compound from the respective guest solvent.

4.1.1. 9,9′-Dichloro-9,9′-bisfluorenyl 4. A mixture of 9,9-dichlorofluorene (7.05 g, 30 mmol) and copper powder (3.81 g) in toluene (50 ml) was heated under reflux for 4 h. After filtration of copper powder, the resultant solution was evaporated to dryness under vacuo and the solid residue was recrystallized from ethyl acetate to give 9,9′-dichloro-9,9′-bisfluorenyl **4**[9] as pale yellow prisms (2.96 g) in 49% yield. Mp 244–245 °C. IR (Nujol): ν_{max} 1603, 1377, 1190, 1034, 929, 849, 737, 695, and 647 cm^{-1}. ^{1}H NMR (DMSO, 70 °C): δ 7.15–7.88 (16H, m, Ar). Anal. Calcd for C$_{26}$H$_{16}$Cl$_2$: C, 78.20; H, 4.04. Found: C, 78.20; H, 4.20.

4.1.2. 2,2′,7,7′,9,9′-Hexachloro-9,9′-bisfluorenyl 5. A mixture of 2,7,9,9-tetrachlorofluorene[9] (0.304 g, 1 mmol) and copper powder (0.127 g) in benzene (20 ml) was heated under reflux for 24 h. After filtration of copper powder, the resultant solution was evaporated to dryness under vacuo and the solid residue was recrystallized from chloroform to give 2,2′,7,7′,9,9′-hexachloro-9,9′-bisfluorenyl **5** as colorless prisms (0.13 g) in 48% yield. Mp 314–315 °C. IR (Nujol): ν_{max} 1580, 1377, 1167, 1075, 956, 810, 773, and 688 cm^{-1}. ^{1}H NMR (DMSO, 100 °C): δ 7.06 (4H, br s, Ar), 7.57 (4H, d, *J*=5.4 Hz, Ar), 7.60 (4H, d, *J*=5.4 Hz, Ar). Anal. Calcd for C$_{26}$H$_{12}$Cl$_6$: C, 58.14; H, 2.25. Found: C, 58.04; H, 2.37.

4.1.3. 2,2′,7,7′-Tetrabromo-9,9′-dichloro-9,9′-bisfluorenyl 6. The powdered crystals of **4** (3.22 g, 8 mmol) were treated with a large excess of bromine in the solid state and left for 12 h at room temperature in the draft. The crude crystals were recrystallized from CCl$_4$ to give 2,2′,7,7′-tetrabromo-9,9′-dichloro-9,9′-bisfluorenyl **6**[9] as colorless needles (5.16 g) in 81% yield. Mp 294–296 °C. IR (Nujol): ν_{max} 1574, 1377, 1249, 1165, 1065, 958, 895, 865, 803, and 766 cm^{-1}. ^{1}H NMR (DMSO, 75 °C): δ 7.65 (12H, br s, Ar). Anal. Calcd for C$_{26}$H$_{12}$Br$_4$Cl$_2$: C, 43.68; H, 1.69. Found: C, 43.66; H, 1.83.

4.1.4. 2,2′,7,7′,9,9′-Hexabromo-9,9′-bisfluorenyl 7. A mixture of 9,9-dichlorofluorene (3.5 g, 15 mmol) and Zn powder (2 g) in xylene (30 ml) was heated under reflux for 24 h. After filtration of Zn powder, the resultant solution was evaporated to dryness under vacuo and the solid residue was recrystallized from ethyl acetate to give bifluorenylidene[10] as red prisms (0.98 g) in 40% yield. The powdered crystals of bifluorenylidene (1.02 g, 3.1 mmol) were treated with a large excess of bromine in the solid state and left for 12 h at room temperature in the draft. The crude crystals were recrystallized from toluene to give 2,2′,7,7′,9,9′-hexabromo-9,9′-bisfluorenyl **7**[9] as colorless prisms in 46% yield. Mp 315–316 °C. IR (Nujol): ν_{max} 1580, 1416, 1377, 1249, 1167, 1167, 1075, 955, 896, 867, 810, 773, and 690 cm^{-1}. ^{1}H NMR (DMSO, 75 °C): δ 7.62 (12H, br s, Ar). Anal. Calcd for C$_{26}$H$_{12}$Br$_6$: C, 38.85; H, 1.50. Found: C, 38.71; H, 1.69.

4.2. X-ray structure determinations

For the host compound **4** and the four inclusion complexes **5**·(*p*-xylene)$_{0.5}$, **6**·CHCl$_3$, **7**·CHCl$_3$, and **7**·1,2-dibromocyclohexane, single crystals of high quality were isolated and their X-ray structures determined. All intensity data were collected on a Nonius Kappa CCD four-circle diffractometer

with Mo Kα radiation and appropriate φ- and ω-scans indicated by program COLLECT.[11] Owing to the generally high X-ray absorption coefficients for these compounds, the crystal specimens were carefully cut to optimize their sizes for intensity data-collection. The specimens were coated with Paratone N oil (Exxon, USA) and cooled in a constant stream of nitrogen vapor at the selected temperature. Intensity data were corrected for absorption with program SADABS.[12] The structures were solved by heavy-atom and direct methods using program SHELX-86[13] and refined by full-matrix least-squares against F^2 using program SHELXL-97.[14] Other programs employed for calculating molecular parameters and visualization included PLATON,[15] ORTEP,[16] and WebLab ViewerPro 3.7.[17]

5. Supplementary material

Crystallographic data have been deposited at the Cambridge Crystallographic Data Centre (deposition numbers CCDC 643320–643324).

Acknowledgements

References and notes

1. *Comprehensive Supramolecular Chemistry*; Atwood, J. L., Davies, J. E. D., MacNicol, D. D., Eds.; Pergamon: Oxford, 1996; Vols. 1–11.
2. Tanaka, K.; Fujimoto, D.; Oeser, T.; Irngartinger, H.; Toda, F. *Chem. Commun.* **2000**, 413–414.
3. Tanaka, K.; Fujimoto, D.; Altreuther, A.; Oeser, T.; Irngartinger, H.; Toda, F. *J. Chem. Soc., Perkin Trans. 2* **2000**, 2115–2120.
4. Tanaka, K.; Fujimoto, D.; Toda, F. *Tetrahedron Lett.* **2000**, *41*, 6095–6099.
5. Tanaka, K.; Caira, M. R. *J. Chem. Res., Synop.* **2002**, 642–643.
6. Marjo, C. E.; Rahman, A. N. M. M.; Bishop, R.; Scudder, M. L.; Craig, D. C. *Tetrahedron* **2001**, *57*, 6289–6293.
7. Rahman, A. N. M. M.; Bishop, R.; Craig, D. C.; Marjo, C. E.; Scudder, M. L. *Cryst. Growth Des.* **2002**, *2*, 421–426.
8. Rahman, A. N. M. M.; Bishop, R.; Craig, D. C.; Scudder, M. L. *Org. Biomol. Chem.* **2004**, *2*, 175–182.
9. Schmidt, J.; Wagner, H. *Liebigs Ann. Chem.* **1912**, *387*, 147–164.
10. Lenoir, D.; Lemmen, P. *Chem. Ber.* **1980**, *113*, 3112–3119.
11. Hooft, R. *COLLECT*; Nonius B.V.: Delft, The Netherlands, 1998.
12. Sheldrick, G. M. *SADABS: Program for Empirical Absorption Corrections*; University of Göttingen: Göttingen, Germany, 1997.
13. Sheldrick, G. M. *Acta Crystallogr.* **1990**, *A46*, 467.
14. Sheldrick, G. M. *SHELXL97*; University of Göttingen: Göttingen, Germany, 1997.
15. Spek, A. L. *Acta Crystallogr.* **1990**, *A46*, C34.
16. Farrugia, L. J. *J. Appl. Crystallogr.* **2000**, *30*, 565.
17. *WebLab ViewerPro 3.7.*; Molecular Simulations: San Diego, CA, 2000.